

25 **Summary statement**

26 *Small ovary* is required for heterochromatin stabilization to repress the expression of
27 transposons and ectopic signaling pathways in the developing ovary.

28

29 **Abstract**

30 Repression is essential for coordinated cell type-specific gene regulation and controlling the
31 expression of transposons. In the *Drosophila* ovary, stem cell regeneration and differentiation
32 requires controlled gene expression, with derepression leading to tissue degeneration and
33 ovarian tumors. Likewise, the ovary is acutely sensitive to deleterious consequences of
34 transposon derepression. The *small ovary* (*sov*) locus was identified in a female sterile screen,
35 and mutants show dramatic ovarian morphogenesis defects. We mapped the locus to the
36 uncharacterized gene *CG14438*, which encodes a zinc-finger protein that colocalizes with the
37 essential Heterochromatin Protein 1 (HP1a). We demonstrate that Sov functions to repress
38 inappropriate cell signaling, silence transposons, and suppress position-effect variegation in
39 the eye, suggesting a central role in heterochromatin stabilization.

40

41 **Introduction**

42 Multicellular organisms rely on stem cells. A combination of extrinsic and intrinsic signals
43 function to maintain the balance between stem cell self-renewal and differentiation needed for
44 tissue homeostasis of stem cell development. The *Drosophila* adult ovary is a well-studied
45 model for development (Fuller and Spradling 2007). It is organized into ~16 ovarioles, which
46 are assembly lines of progressively maturing egg chambers. At the anterior tip of each ovariole
47 is a structure called the germarium, harboring 2–3 germline stem cells (GSCs), which sustain
48 egg production throughout the life of the animal. Surrounding the GSCs and their cystoblast

49 daughters is a stem cell niche, a collection of nonproliferating somatic cells composed of
50 terminal filament and cap cells. Like the GSCs, somatic stem cells divide to produce new stem
51 cells and escort cells, which encase the germline. Each cystoblast is fated to differentiate and
52 will undergo four rounds of cell division with incomplete cytokinesis to produce a germline cyst
53 interconnected by the fusome, a branched cytoskeletal structure. Germline cysts are
54 surrounded by two escort cells. Toward the posterior of the germarium, a monolayer of somatic
55 follicle cells replaces the escort cells to form an egg chamber.

56 Egg chamber development requires the careful coordination of distinct germline and
57 somatic cell populations through signaling within a complex microenvironment. For example,
58 extrinsic transducers and signals including Jak/Stat and the BMP homolog, Decapentaplegic
59 (Dpp), are required to maintain the proliferative potential of GSCs (Bausek 2013; Gilboa 2015;
60 S. Chen, Wang, and Xie 2011). Oriented divisions displace the primary cystoblast cell away
61 from the stem cell signals and permit the expression of differentiation factors, such as *bag of*
62 *marbles* (*bam*). The importance of Bam is revealed in *bam* loss-of-function mutants, which
63 have tumorous germaria filled with undifferentiated germline cells containing dot
64 spectrosomes, the dot-fusome structure characteristic of GSCs and primary cystoblasts as a
65 result of complete cytokinesis (Lin and Spradling 1995; D. McKearin and Ohlstein 1995). Thus,
66 germline differentiation requires the repression and activation of cell signaling pathways.

67 Dynamic changes in chromatin landscapes within germline and somatic cells are critical
68 for oogenesis and contribute to the regulated gene expression required for tissue homeostasis
69 (Barton et al. 2016; X. Li et al. 2017; Börner et al. 2016; Peng et al. 2016; Soshnev et al. 2013;
70 McConnell, Dixon, and Calvi 2012). Nucleosomes generally repress transcription by competing
71 for DNA binding with transcription factors (Lorch and Kornberg 2017; Kouzarides 2007;

72 Jenuwein and Allis 2001). The reinforcement of repression depends largely on histone
73 modifications. For example, the activities of both the H3K9 methyltransferase SETDB1,
74 encoded by *eggless* (*egg*) (Wang et al. 2011; Clough et al. 2007; Clough, Tedeschi, and
75 Hazelrigg 2014), and the H3K4 demethylase encoded by *lysine-specific demethylase 1* (Di
76 Stefano et al. 2007; Rudolph et al. 2007; Eliazer, Shalaby, and Buszczak 2011; Eliazer et al.
77 2014) are required in the somatic cells of the germarium for GSC maintenance, normal
78 patterns of differentiation, and germline development. Genomewide profiling hints at a
79 progression from open chromatin in stem cells to a more closed state during differentiation (T.
80 Chen and Dent 2014). Disrupting this progressive repression in the ovary is predicted to
81 contribute to stem cell overproliferation and defective oogenesis.

82 There are other roles for regulated chromatin states in oogenesis. The propensity of
83 transposons to mobilize in gonads is countered by host responses, such as induced
84 heterochromatin formation, to repress transposon activity. The proximity of condensed
85 heterochromatin also dampens the activity of genes and transgenes (Elgin and Reuter 2013).

86 Originally described over 40 years ago (J. D. Mohler 1977), the *small ovary* (*sov*) locus
87 is associated with a range of mutant phenotypes including disorganized ovarioles, egg
88 chamber fusions, undifferentiated tumors, and ovarian degeneration (Wayne et al. 1995). In
89 the present work, we define the molecular identify and function of Sov. We demonstrate *sov*
90 encodes an unusually long C₂H₂ zinc-finger (ZnF) nuclear protein. Previous work suggested
91 Sov may complex with the conserved Heterochromatin-Protein 1a (HP1a) (Alekseyenko et al.
92 2014), encoded by *Su(var)205* and critical for heterochromatin formation (James and Elgin
93 1986; Eissenberg et al. 1990; Clark and Elgin 1992). RNA-seq analysis showed that *sov*
94 activity is required in the ovary to repress the expression of a large number of genes and

95 transposons. Additionally, Sov functions as a dominant suppressor of position-effect
96 variegation (PEV) in the eye, similar to HP1a (Elgin and Reuter 2013). Moreover, Sov and
97 HP1a colocalize in the nucleus. These data indicate that Sov is a novel repressor of gene
98 expression involved in heterochromatization.

99

100 **Results**

101 *small ovary is CG14438*

102 To refine previous mapping of *sov*, we used complementation of female sterile and lethal *sov*
103 mutations with preexisting and custom-generated deficiencies, duplications, and transposon
104 insertions (J. D. Mohler 1977; D. Mohler and Carroll 1984; Wayne et al. 1995). Our results (Fig
105 1A, B) suggested that either the protein-coding *CG14438* gene or the intronic, noncoding
106 *CR43496* gene is *sov* since the locus mapped to the noncomplementing deletion *Df(1)sov*.
107 Rescue of female sterility and/or lethality of *sov*², *sov*^{ML150}, *sov*^{EA42} and *Df(1)sov* with
108 *Dp(1;3)sn*^{13a1} (molecularly undefined, not shown), *Dp(1;3)DC486*, and *PBac{GFP-*sov*}*
109 confirmed our mapping. We could not replicate separability of *sov*^{EA42} sterility and lethality with
110 *Dp(1;3)sn*^{13a1} (Wayne et al. 1995). Female sterile and lethal alleles of *sov* map identically.

111 We performed genome sequencing to determine if the lesions in *sov* alleles occur in
112 *CG14438* or *CR43496* (Table S1). While *CR43496* contained three polymorphisms relative to
113 the reference genome, we identified the same polymorphisms in all *sov* mutant and control
114 lines. Thus, *CR43496* is unlikely to be *sov*. In contrast, we found disruptive mutations in
115 *CG14438* (Fig 1C), which encodes an unusually long, 3,313-residue protein with 21 C₂H₂ ZnFs
116 and multiple nuclear localization motifs and coiled-coil regions (Fig 1C). We identified a
117 nonsense mutation (G to A at position 6,764,462) in the *CG14438* open reading frame of

118 *sov*^{EA42} which is predicted to truncate the *sov* protein before the ZnF domains. We found a
119 frameshift insertion (T at position 6,769,742) located towards the end of *CG14438* in *sov*² that
120 encodes 30 novel residues followed by a stop codon within the C-terminal ZnF and removes
121 the terminally predicted NLS (Fig 1C). We found a missense mutation (C to G at position
122 6,763,888) in *sov*^{ML150} that results in a glutamine to glutamate substitution within a predicted
123 coiled-coil domain. While this is a conservative substitution and glutamate residues are
124 common in coiled-coil domains, glutamine to glutamate substitutions are especially disruptive
125 in the coiled-coil region of the sigma transcription factor (Hsieh, Tintut, and Gralla 1994). We
126 conclude that *CG14438* encodes *sov*.

127

128 *sov* is highly expressed in the ovary

129 To determine where *sov* is expressed and if it encodes multiple isoforms, we analyzed its
130 expression in adult tissues by RNA-seq. We noted that *sov* is broadly expressed as a single
131 mRNA isoform, with highest expression in ovaries (Fig 1D). The modENCODE (Graveley et al.
132 2011; J. B. Brown et al. 2014) and FlyAtlas (Robinson et al. 2013; Leader et al. 2018)
133 reference sets show a similar enrichment in the ovary and early embryos. The enrichment of
134 *sov* in the ovary is consistent with its reported oogenesis phenotypes.

135 To determine where *Sov* is expressed in the ovary, we generated a GFP-tagged
136 transgene (GFP-*Sov*) sufficient to rescue ovary degeneration in *sov* mutants. Examination of
137 the distribution of GFP-*Sov* in developing egg chambers (Fig 2A) revealed *Sov* localization in
138 several cell types. By pairing localization analysis of *Sov* with antibodies recognizing *Vasa*
139 (*Vas*) to label the germline, we observed particularly striking nuclear localization of *Sov*
140 surrounded by perinuclear *Vas* in the germline cells within region 1 of the germarium, with

141 highest levels evident within the GSCs (dashed circles; Fig 2B). Using Traffic jam (Tj) to label
142 the soma highlighted nuclear enrichment of Sov in the Tj-positive somatic and follicle stem
143 cells (dashed ovals; Fig 2C). These data indicate that Sov is enriched in the germline and
144 somatic cells of the ovary, including both stem cell populations.

145

146 *Sov is required in the soma and germline for oogenesis*

147 To examine *sov* function in the germarium, we compared a strong allelic combination,
148 *sov^{EA42}/sov²*, to cell-type specific knockdown of *sov* using a UAS short hairpin *sov* RNAi
149 construct (P{TRiP.HMC04875}; hereafter, *sov^{RNAi}*). The germaria of heterozygous *sov* females
150 are wild type (Fig 3A), but *sov* mutants often show an ovarian tumor phenotype, with greater
151 than the expected number of germ cells with dot spectrosomes (Fig 3B), indicating that germ
152 cells undergo complete cytokinesis. Ovarian tumors were observed in ~40% of *sov* mutants
153 (N=12/31 *sov^{EA42}/sov²* egg chambers versus N=0/47 controls). These findings are consistent
154 with GSC hyperproliferation and/or failed differentiation. We also observed tumors and nurse
155 cell nuclei residing within common follicles (Fig 3B) in about one-third of *sov* mutants (N=11/31
156 *sov^{EA42}/sov²* versus N=0/24 in controls). This phenotype occurs when follicle cells either fail to
157 separate egg chambers, or where those chambers fuse (Goode, Wright, and Mahowald 1992).
158 Consistently, disorganization of the follicle cell monolayer was also observed (dashed lines,
159 Fig 3B). In older *sov* ovaries, we also observed extensive cell death (Fig S1). Additionally, we
160 found that rare *sov^{EA42}/Y* males that escaped lethality had no germ cells (Fig S2). Thus, *sov*
161 functions widely.

162 To examine cell-type specific functions of *sov*, we used *tj-GAL4* to express *sov^{RNAi}* (or
163 *mCherry^{RNAi}* controls) in somatic escort and follicle cells and *nanos-GAL4* (*nos-GAL4*) to

164 express RNAi in the germline. Relative to the controls, the *tj>sov^{RNAi}* germaria (Fig 3C, D) were
165 abnormal, showing ovarian tumor phenotypes similar to those seen in *sov* mutants. Germaria
166 were often filled with germline cells with dot spectrosomes and the follicle cells encroached
167 anteriorly. Similar results were also observed using other somatic drivers (*c587-GAL4* and *da-*
168 *GAL4*). Interestingly, *nos>sov^{RNAi}* did not impair germarium morphology (Fig 3E, F) and egg
169 chambers representing all 14 morphological stages of oogenesis appeared phenotypically
170 normal. However, eggs produced from *nos>sov^{RNAi}* mothers arrested during early
171 embryogenesis, indicating that maternal *sov* is required for embryonic development. While *sov*
172 expression patterns and germline RNAi suggest that *sov* is deployed in both the soma and
173 germline, Wayne et al. (1995) reported *sov* to be somatic cell dependent. To further address a
174 requirement for *sov* in the germline, we conducted germline clonal analysis. Depletion of *sov*
175 from the germline results in an agametic phenotype (Fig S3). Additionally, *sov^{RNAi}* resulted in
176 embryonic germline defects in a high-throughput study (Jankovics et al. 2014). Taken together,
177 these data indicate that there are both somatic and germline requirements for *sov* in
178 oogenesis.

179 To explore the differentiation of the germline further, we examined the distribution of
180 Bam, which is expressed in germarium region 1 germ cells (D. M. McKearin and Spradling
181 1990; D. McKearin and Ohlstein 1995; Ohlstein and McKearin 1997). In the absence of Bam,
182 germ cells hyperproliferate, resulting in tumors composed of 2-cell cysts. Given the prevalence
183 of undifferentiated tumorigenic germ cells upon somatic *sov^{RNAi}* knockdown, we asked if *sov*
184 has a nonautonomous role in promoting Bam expression in germ cells. Indeed, somatic
185 knockdown of *sov* results in significantly less Bam expressed in germ cells relative to controls
186 (Fig 3G, H; Fig S4). Both *tj-GAL4>sov^{RNAi}* and *c587-GAL4>sov^{RNAi}* resulted in a strong

187 decrease in Bam expression. Germline depletion of *sov* did not alter Bam expression (Fig S4).
188 The reduction in Bam expression in the germline is consistent with a nonautonomous role of
189 *Sov* function in the soma for differentiation signals directed to the germline.

190 To examine the defective follicle encapsulation of the germline cysts following *sov*
191 depletion, we used the oocyte-specific expression of Oo18 RNA binding protein (Orb) (Lantz et
192 al. 1994) to count the number of oocytes per cyst. Orb specifies the future single oocyte at the
193 posterior of the egg chamber in control egg chambers (Fig 3I, Fig S2D). Somatic depletion of
194 *sov* resulted in examples of both egg chambers with either too many oocytes (Fig 3J) or no
195 oocytes (Fig 3K, Fig S4). In a wild type 16-cell germline cyst, one of the two cells that has four
196 ring canals becomes the oocyte, and this feature can be used to determine if extra germline
197 divisions had occurred in cysts, or if multiple cysts were enveloped by the follicle cells. We saw
198 that the egg chambers with multiple Orb⁺ cells always had more than 16 germ cells, and in the
199 representative example shown, all three Orb⁺ cells had four ring canals, indicating that egg
200 chamber fusion had occurred (Fig 3J). Taken together, we conclude that *Sov* functions in the
201 soma to ensure proper differentiation of the germline.

202

203 *Sov represses gene expression in the ovary*

204 To provide mechanistic insights into the function of *Sov*, we performed transcriptome profiling
205 using triplicated Poly-A⁺ RNA-seq analyses of ovaries from *sov*, *sov*^{RNAi}, and control females.
206 The gene expression profiles of ovaries from sterile females were markedly different from
207 controls, primarily due to derepression in the mutants (Fig 4A; Table S2). Among genes
208 showing differences in expression (FDR *p*_{adj} < 0.05), we found 1,752 genes with >4-fold
209 increased expression in mutants, while there were only 172 genes with >4-fold decreased

210 expression (Table S3). To explore where these derepressed genes are normally expressed,
211 we examined their expression in other female tissues and in testes in a set of quadruplicated
212 RNA-seq experiments (Fig 4B). Many of the genes suppressed by Sov in ovaries were highly
213 expressed in other female tissues, but not testes, indicating that wild type Sov prevents ectopic
214 gene expression.

215 To determine what types of genes are derepressed in *sov* mutants, we performed Gene
216 Ontology (GO)(Gene Ontology Consortium 2015) term analysis (Fig S5; Table S4). The genes
217 with lower expression in *sov* mutants had only a few significant GO terms that were
218 predominantly oogenic in nature (as expected given the general lack of mature eggs). For
219 example, there was poor expression of the chorion genes that are required to build the
220 eggshell (Orr-Weaver 1991), as well as genes required for follicle cell development. In
221 contrast, the derepressed genes in *sov* mutants showed a significant enrichment of cell
222 signaling GO terms, including neuronal communication. We found that many genes repressed
223 by Sov in the ovary, such as the *heartless (htl)* locus, which encodes a FGFR tyrosine kinase
224 receptor important for neuron/glia communication (Stork et al. 2014), are indeed expressed in
225 the head (Fig 4C). These results suggest that *sov* normally functions to repress a host of
226 signaling pathways. Derepressed signaling in *sov* mutants is likely catastrophic for
227 communication between various somatic cells and the germline during egg chamber
228 development and could explain the variety of mutant ovarian phenotypes.

229 The general repressive role of *sov* was also revealed by a dramatic and coherent
230 elevation of transposon expression in the mutants (Fig 4D; Table S3). Of the 138 transposable
231 element classes detected in our gene expression profiling of *sov* mutants and controls, 91 had
232 increased expression (FDR $p_{adj} < 0.05$) >4-fold in *sov* mutants, while none had >4-fold

233 decreased expression. The DNA, LINE, and LTR families of transposable elements were all
234 derepressed in *sov* mutants. Interestingly, somatic knockdown of *sov* resulted in the most
235 dramatic derepression of the *gypsy* and *copia* classes of transposons, which are *Drosophila*
236 retroviruses that develop in somatic cells and are exported to the developing germline
237 (Yoshioka et al. 1990). Thus, wild type *sov* may be important to protect the germline from
238 infection. Equally interesting, germline knockdown resulted in the greatest derepression of the
239 *HeT-A*, *TAHRE*, and *TART* transposons that compose the telomere (Mason, Frydrychova, and
240 Biessmann 2008). This finding suggests that the general role of *sov* in silencing transposon
241 expression includes control of both transposon functions necessary for normal cellular
242 metabolism, exemplified by the telomere transposons, as well as detrimental activities of
243 retrovirus-like elements. In addition to widespread deregulation of signaling and development
244 pathways in *sov* mutants, transposon dysgenesis may contribute to the severe ovarian
245 development defects in *sov* mutants.

246

247 *Sov is a suppressor of PEV and colocalizes with HP1*

248 The repressive function of *Sov* is reminiscent of *HP1a* function as a general repressor of gene
249 expression. *HP1a* was first characterized in *Drosophila* as a suppressor of *PEV*, a process that
250 reduces gene expression due to spreading of heterochromatin into a gene region (Clark and
251 Elgin 1992). To test the hypothesis that *sov* negatively regulates gene expression by
252 promoting heterochromatin formation, we examined the role of *sov* in *PEV* in the eye, where
253 patches of *white*⁺ (red pigmented) and *white*⁻ (not red pigmented) eye facets are easily
254 observed (Fig 5A). If, like *HP1a*, *Sov* represses gene expression by promoting
255 heterochromatin formation (Eissenberg et al. 1990), then it should suppress *PEV*, which is

256 scored by increased eye pigmentation. We obtained five different variegating w^+ transgene
257 insertions associated with either the heterochromatic pericentric region of chromosome arm 2L
258 or spread along the length of the heterochromatin-rich chromosome 4. In control animals,
259 these insertions show a characteristic eye variegation pattern (Fig 5B). Consistent with the
260 allelic strengths seen in previous experiments, the weak sov^2 allele did not suppress PEV (Fig
261 5C), but the stronger sov^{ML150} , sov^{EA42} , and $Df(1)sov$ mutations dominantly suppressed PEV
262 (Fig 5D–F). These data demonstrate a role for Sov in heterochromatin formation.

263 The strong repressive function of Sov is reminiscent of HP1a. Prior in vitro work
264 suggests Sov may complex with HP1a (Alekseyenko et al. 2014). To determine if Sov and
265 HP1a associate in vivo, we followed HP1a-RFP and GFP-Sov localization in 1–2 hr live
266 embryos. During *Drosophila* embryogenesis, nuclei undergo rapid synchronous nuclear
267 divisions prior to cellularization at cleavage division/nuclear cycle (NC) 14 (Foe and Alberts
268 1983). HP1a and Sov colocalized in all NC 10–12 embryos we examined (Fig 6A; N=7
269 embryos). During prophase, both HP1a and Sov were enriched in regions of condensed DNA
270 (Fig 6A, 4:30). Whereas low levels of HP1a decorated DNA throughout division, Sov was
271 depleted during mitosis (Fig 6A, 10:00 and 11:10). Upon reentry into interphase, Sov
272 localization to nuclei resumed and was coincident with HP1a. Formation of heterochromatin is
273 contemporaneous with or slightly precedes HP1a apical subnuclear localization in NC 14
274 (Rudolph et al. 2007; Yuan and O'Farrell 2016). At this stage, we observed a strong
275 colocalization of HP1a and Sov. Measuring the distribution of HP1a and Sov (Fig 6B, B')
276 confirmed high levels of colocalization within HP1a subnuclear domains (Fig 6C, shaded
277 region). These data support the idea that HP1a and Sov are deposited maternally where they
278 assemble into a complex.

279

280 **Discussion**

281 Sov is a novel heterochromatin-associated protein

282 Genomes contain large blocks of DNA of potentially mobile transposons and immobile mutated
283 derivatives (Vermaak and Malik 2009). The cell keeps these transposons from wreaking havoc
284 on the genome by actively suppressing their expression through condensation into
285 heterochromatin. However, some tightly regulated expression from heterochromatin is required
286 for normal cellular function. For example, the telomeres of *Drosophila* are maintained by
287 transposition of mobile elements from heterochromatic sites (Mason, Frydrychova, and
288 Biessmann 2008), and histone and rRNA genes are located within heterochromatic regions
289 (Yasuhara and Wakimoto 2006). Weakening of heterochromatin by suppressors of variegation
290 results in derepression of gene expression at the edges of heterochromatin blocks, suggesting
291 that the boundaries between repressed and active chromatin can expand and contract (Weiler
292 and Wakimoto 1995; Reuter and Spierer 1992). HP1a, encoded by *Su(var)205*, is a central
293 component of heterochromatin (Ebert et al. 2006) that shows the same strong suppression of
294 variegation that we observed in *sov*/+ flies. Similarly, HP1a is also required to repress the
295 expression of transposons (Vermaak and Malik 2009).

296 Repression is often stable and emerging themes suggest a robust set of activities,
297 rather than a single component, maintain a chromatin state. For example, long-term repression
298 is stabilized with complexes, such as the repressive Polycomb Group (PcG) which provides an
299 epigenetic memory function (Kassis, Kennison, and Tamkun 2017). In order to create a stable
300 epigenetic state, PcG complexes have subunits that modify histones and bind these
301 modifications. Chromatin tethering of PcG complexes also involves DNA-binding proteins,

302 such as the YY1-like ZnF protein Pleiohomeotic (Pho), which further reinforce localization. The
303 DNA anchor proteins in PcG complexes are at least partially redundant with the histone-
304 binding components (J. L. Brown et al. 2003), suggesting that localization is robust due to
305 multiple independent localization mechanisms.

306 In mammals, HP1a also has both histone binding and DNA anchoring requirements.
307 DNA anchoring is provided by a family of KRAB ZnF proteins that have undergone a massive
308 radiation during evolution (Yang, Wang, and Macfarlan 2017; Ecco, Imbeault, and Trono
309 2017). KRAB proteins are essential for repression of transposons and more generally for a
310 properly regulated genome. The KRAB family members use a KRAB-Associated Protein
311 (KAP1) adapter protein to associate with HP1a and the SETDB1 methylase that modifies
312 histones to enable HP1a binding (Fig 7). Although KRAB proteins have not been identified in
313 *Drosophila*, the *Drosophila bonus* (*bon*) gene encodes a KAP1 homolog (Beckstead et al.
314 2005). *Drosophila* also has a SETDB1 encoded by *egg*, and loss of *egg* results in ovarian
315 phenotypes reminiscent of those observed in *sov* loss-of-function females (Clough et al. 2007;
316 Clough, Tedeschi, and Hazelrigg 2014; Wang et al. 2011). Like *sov* and *HP1a*, *bon* is a
317 modifier of variegation, raising the possibility that they collectively coordinate gene regulation.
318 In support of this hypothesis, *Bon*, *Sov*, and *Egg* were all identified in the same biochemical
319 complex as HP1a (Alekseyenko et al. 2014). It is tempting to speculate that the single very
320 long and ZnF-rich *Sov* protein plays the same direct binding role as the large family of KRAB
321 ZnF proteins in mammals (Fig 7). If *Sov* uses subsets of fingers to bind DNA, it could localize
322 to many different sequences in a combinatorial fashion. Additionally, the complex containing
323 *Sov* and HP1a also contains RNA (Alekseyenko et al. 2014) and could act as a tether via a
324 series of RNA intermediates as occurs in sex chromosome inactivation, for example (J. T. Lee

325 2009). As in the case of Pho in the PcG complexes, Sov might be a robustness factor rather
326 than an absolute requirement, as we did not observe gross delocalization of HP1a following
327 *sov*^{RNAi} (not shown). Further work will be required to fully understand the relationship between
328 Sov and HP1a.

329

330 Repression by Sov promotes germline differentiation

331 The fact that there have been many female sterile alleles of *sov* suggests that the ovary
332 is particularly sensitive to reduced *sov* activity. The female sterility phenotype is complex and
333 somewhat variable, but partial *sov* loss of function is characterized by somatic-dependent
334 differentiation defects. Stronger alleles also show a germline-dependent block in development
335 and lethality. While *sov* functions seem diverse, the locus expresses a single major isoform,
336 and Sov seems to be consistently located in the nucleus. We propose that the
337 multifunctionality of Sov may be attributed to a single mechanism wherein Sov helps control
338 heterochromatin formation required to repress ectopic gene expression and tissue-
339 inappropriate responses in the ovary and repress transposons (Fig 7).

340 We observed dramatic derepression of transposons in *sov* mutants. Consistent with our
341 observations, Czech et al (2013) reported a role of *sov* in transposon repression in a
342 genomewide RNAi screen. That work raised the possibility that transposon repression by Sov
343 occurs via the piRNA pathway (Brennecke et al. 2007; Yin and Lin 2007; Teixeira et al. 2017).
344 However, genes involved more strictly with transposable element regulation, such as Piwi, do
345 not have strong dosage effects on PEV (Gu and Elgin 2013), while *sov* and *HP1a/Su(var)205*
346 do. This distinction suggests that Sov has a more general effect on heterochromatin, rather
347 than specificity for transposon repression. Germline knockdown of HP1a results in a strong

348 derepression of telomeric transposons (Teo et al. 2018), just like Sov. This is suggested to be
349 due to a reduction in piRNAs specifically targeting these transposons and thus interplay
350 between the piRNA pathway, Sov, and HP1a remains possible.

351

352 Conclusions

353 Our data show that *sov* encodes a repressor of gene expression and transposons in the
354 ovary. In the absence of *sov*, genes that are normally expressed at very low levels in the
355 ovary, are activated. These same genes show dynamic patterns of expression in other adult
356 tissues, suggesting that they are derepressed in the absence of Sov. The failure to restrict
357 gene expression results in a range of phenotypes including ovarian tumors, defective
358 oogenesis, and tissue degeneration. These data support the idea that Sov encodes a novel
359 and essential protein that is generally repressive, likely via interactions with HP1a.

360

361 **Materials and Methods**

362 We have adopted the FlyBase-recommended resources table which includes all genetic,
363 biological, cell biology, genomics, manufactured reagents and algorithmic resources used in
364 this study (Table S5).

365

366 Flies and genetics

367 *sov* was defined by three X-linked, female sterile mutations including *sov*², which
368 mapped to ~19 cM (Mohler 1977; Mohler and Carroll 1984), refined to 6BD (Wayne *et al.*
369 1995). We used existing and four custom-made deletions (*Df(1)BSC276*, *BSC285*, *BSC286*
370 and *BSC297*) to map *sov* to the 4-gene *CG14438–shf* interval (Fig. 1; Table S5). *sov*

371 mutations complemented shf^2 , but not $P\{SUPor-P\}CG14438^{KG00226}$ or $P\{GawB\}NP6070$,
372 suggesting $CG14438$ or $CR43496$ is *sov*, which we confirmed by generating $Df(1)sov$
373 (X:6756569..6756668;6770708) from FLP crossover between $P\{XP\}CG14438^{d07849}$ and
374 $PBac\{RB\}e03842$ (Parks et al. 2004; Cook et al. 2012) to remove only those two genes.

375 We used the dominant female sterile technique for germline clones (Chou and Perrimon
376 1996). Test chromosomes, that were free of linked lethal mutations by male viability (sov^2) or
377 rescue by $Dp(1;3)DC486$ (sov^{EA42} and $Df(1)sov$), were recombined with $P\{ry^{+t7.2}=neoFRT\}19A$,
378 and verified by complementation tests and PCR. We confirmed $P\{ry^{+t7.2}=neoFRT\}19A$
379 functionality by crossing to $P\{w^{+mC}=GMR-hid\}SS1, y^1 w^* P\{ry^{+t7.2}=neoFRT\}19A; P\{w^{+m*}=GAL4-$
380 $ey.H\}SS5, P\{w^{+mC}=UAS-FLP.D\}JD2$ and scoring for large eye size. We crossed females with
381 FRT chromosomes to $P\{w^{+mC}=ovoD1-18\}P4.1, P\{ry^{+t7.2}=hsFLP\}12, y^1 w^{1118} sn^3$
382 $P\{ry^{+t7.2}=neoFRT\}19A/Y$ males for 24 hours of egg laying at 25°C. We heat-shocked for 1hr at
383 37°C on days 2 and 3. We dissected females (5d posteclosion) to score for ovo^{D1} or wild type
384 morphology.

385 We generated $PBac\{GFP-sov\}$ from P[acman] BAC clone CH322-191E24 (X:6753282–
386 6773405) (Venken et al. 2009) grown in the SW102 strain (Warming et al. 2005). In step one,
387 we integrated the positive/negative marker CP6-RpsL/Kan (CP6 promoter with a bi-cistronic
388 cassette encoding the RpsL followed by the Kan), PCR-amplified with primers N-CG14438-
389 CP6-RN-F and -R between the first two codons of *sov*, and selected (15 µg/ml Kanamycin)
390 We integrated at the *galK* operon in DH10B bacteria using mini-lambda-mediated
391 recombineering (Court et al. 2003). We amplified DH10B::CP6-RpsL/Kan DNA using primers
392 N-CG14438-CP6-RN-F and -R. Correct events were identified by PCR, as well as resistance
393 (15 µg/ml Kanamycin) and sensitivity (250 µg/ml Strep). In step two, we replaced the selection

394 markers with a multi-tag sequence (Venken et al. 2011), tailored for N-terminal tagging (N-tag)
395 and counter-selected (250 µg/ml Strep). The N-tag (3xFlag tag, TEV protease site, StrepII tag,
396 superfolder GFP, FIAsh tetracysteine tag, and flexible 4xGlyGlySer (GGs) linker) was
397 *Drosophila* codon optimized in a R6Ky plasmid. We transformed plasmid into EPI300 for copy
398 number amplification. We confirmed correct events by PCR and Sanger DNA sequencing.
399 Tagged P[acman] BAC clone DNA was injected into $y^1 M\{vas-int.Dm\}ZH-2A w^*$; $PBac\{y+-attP-$
400 $3B\}VK00033$ embryos, resulting in w^{1118} ; $PBac\{y[+mDint2] w^{+mC}=FTSF.GFP-sov\}VK00033$.

401

402 Microscopy

403 We fixed ovaries in 4 or 5% EM-grade paraformaldehyde in PBS containing 0.1 or 0.3%
404 Triton X-100 (PBTX) for 10–15min, washed 3x 15 min in PBTX, and blocked >30min in 2%
405 normal goat serum, 0.5-1% bovine serum albumin (BSA) in PBS with 0.1% Tween-20 or 0.1%
406 Triton X-100. Antibodies and DAPI were diluted into blocking buffer. We incubated in primary
407 antibodies overnight at 4°C and secondaries 2–3hr at room temperature. Embryos (1–2 hr)
408 were prepared for live imaging in halocarbon oil (Lerit et al. 2015). We imaged ovaries and
409 embryos using a Nikon Ti-E system or Zeiss LSM 780 microscope and eyes with a Nikon SMZ.

410

411 DNA-Seq

412 Genomic DNA was extracted from 30 whole flies per genotype (Huang, Rehm, and
413 Rubin 2009)(Sambrook and Russell 2006) to prepare DNA-seq libraries (Nextera DNA Library
414 Preparation Kit). We used 50 bp, single-end sequencing (Illumina HiSeq 2500, CASAVA base
415 calling). Sequence data are available at the SRA (SRP14438). We mapped DNaseq reads to
416 FlyBase r6.16 genome with Hisat2 (-k 1 --no-spliced-alignment)(Kim, Langmead, and Salzberg

417 2015). We used mpileup and bcftools commands from SAMtools within the genomic region
418 X:6756000–6771000 (H. Li et al. 2009; H. Li 2011) for variant calling and snpEFF to determine
419 the nature of variants in *sov* mutants (Cingolani et al. 2012).

420

421 RNA-seq

422 Stranded PolyA+ RNA-seq libraries from *sov* and control ovaries (Table S5) were
423 created (H. Lee, Cho, et al. 2016) and are available at GEO (GSE113977). We extracted total
424 RNA (Qiagen RNeasy Mini Kit) in biological triplicate from 15 ovaries (4–5d posteclosion) and
425 used 200 ng with 10 pg of ERCC spike-in control RNAs (pools 78A or 78B) for libraries (Jiang
426 et al. 2011; Zook et al. 2012; Pine et al. 2016; H. Lee, Pine, et al. 2016). We used 50 bp,
427 single-end sequencing as above. Tissue expression analysis are from GEO accession
428 GSE99574, a resource for comparing gene expression patterns.

429 We mapped RNA-seq reads to FlyBase r6.21 with Hisat2 (-k 1 --rna-strandness R --dta)
430 (Kim, Langmead, and Salzberg 2015). We determined read counts for each attribute of the
431 FlyBase r6.21 GTF file (with ERCC and transposable element sequences), with HTSeq-count
432 (Anders, Pyl, and Huber 2015). Transposon sequences were from the UCSC Genome
433 Browser RepeatMasker track (Casper et al. 2018; Smit, Hubley, and Green 2013-2015).

434 We conducted differential expression analysis with DESeq2 (pAdjustMethod = "fdr")
435 (Love, Huber, and Anders 2014). We removed genes with read counts <1 and read counts for
436 transposable elements with >1 locations were summed for the DESeq2 analysis. $Df(1)_{sov/sov^2}$
437 replicate 3 and sov^2/w^{1118} replicate 1 were failed. For *sov* mutant vs. control DESeq2 analysis,
438 all *sov* mutants were compared to all wild type controls. For tissue types, we compared each

439 sexed tissue to sexed whole organism. We used reads per kb per million reads (RPKM) for
440 gene-level expression.

441 For heatmaps, we calculated Euclidean distance, performed hierarchical cluster
442 analysis (agglomeration method = Ward), and mean-subtracted scaled across genotypes.
443 Mean sample RPKM correlation values (Table S1) were calculated by `cor.test()` function with
444 Pearson correlation coefficient in R (R Core Team 2017). We represented derepressed genes
445 as mean-subtracted scaled values across tissues in the heatmap (Table S6).

446 For read density tracks, replicate raw read files were combined. Bedgraph files were
447 created with bedtools genomecov (Quinlan and Hall 2010) visualized on the UCSC genome
448 browser (Kent et al. 2002). Tracks were scaled by the number of reads divided by total reads
449 per million.

450 We used ClueGO (Bindea et al. 2009), with Cytoscape (Shannon et al. 2003) for one-
451 sided enrichment analysis (see Table S4).

452 Images were assembled using ImageJ and Photoshop. We used ROI tool in ImageJ,
453 plotted/analyzed image data (Microsoft Excel and GraphPad Prism), and calculated
454 significance by D'Agostino and Pearson normality tests, followed Student's two-tailed t-test or
455 Mann-Whitney tests.

456

457 **Acknowledgements**

458 Stocks obtained from the Bloomington Drosophila Stock Center (NIH P40OD018537) and
459 Drosophila Genomics and Genetic Resources at the Kyoto Institute of Technology were used
460 in this study. Monoclonal antibodies were obtained from the Developmental Studies Hybridoma
461 Bank, created by the NICHD of the NIH and maintained at The University of Iowa, Department

462 of Biology, Iowa City, IA 52242. Sequencing was performed by the NIDDK Genomics Core,
463 under the direction of Harold Smith. Genetic and genomic information was obtained from
464 FlyBase. This work utilized the computational resources of the NIH HPC Biowulf cluster
465 (<http://hpc.nih.gov>). We thank BACPAC resources for plasmids, Norbert Perrimon for the
466 *sov*^{EA42} stock and Don Court, Neal Copeland, and Nancy Jenkins for the recombineering
467 strain. We thank Astrid Haase, Nasser Rusan, David Katz, and members of the Oliver and
468 Lerit labs for stimulating discussions. Particular thanks go to Stacy Christensen and Kimberley
469 Cook for generating and characterizing the *sov* deletions. This research was supported in part
470 by the Intramural Research Program of the NIH, National Institute of Diabetes and Digestive
471 and Kidney Diseases (NIDDK) to BO. DAL and EAC were supported by NIH grant
472 5K22HL126922-02 (DAL). LB was supported by the NIH Graduate Partners Program. KJTV
473 was supported by Baylor College of Medicine, the Albert and Margaret Alkek Foundation, the
474 McNair Medical Institute at The Robert and Janice McNair Foundation, the March of Dimes
475 Foundation (#1-FY14-315), the Foundation for Angelman Syndrome Therapeutics (FT2016-
476 002), the Cancer Prevention and Research Institute of Texas (R1313), and NIH grants
477 (1R21HG006726, 1R21GM110190, 1R21OD022981, and R01GM109938). CW and KRC were
478 supported by the Office of the NIH Director, the National Institute of General Medical Sciences
479 and the National Institute of Child Health and Human Development (P40OD018537). KRC was
480 supported by the National Center for Resource Resources (R24RR014106) and the National
481 Science Foundation (DBI-9816125).

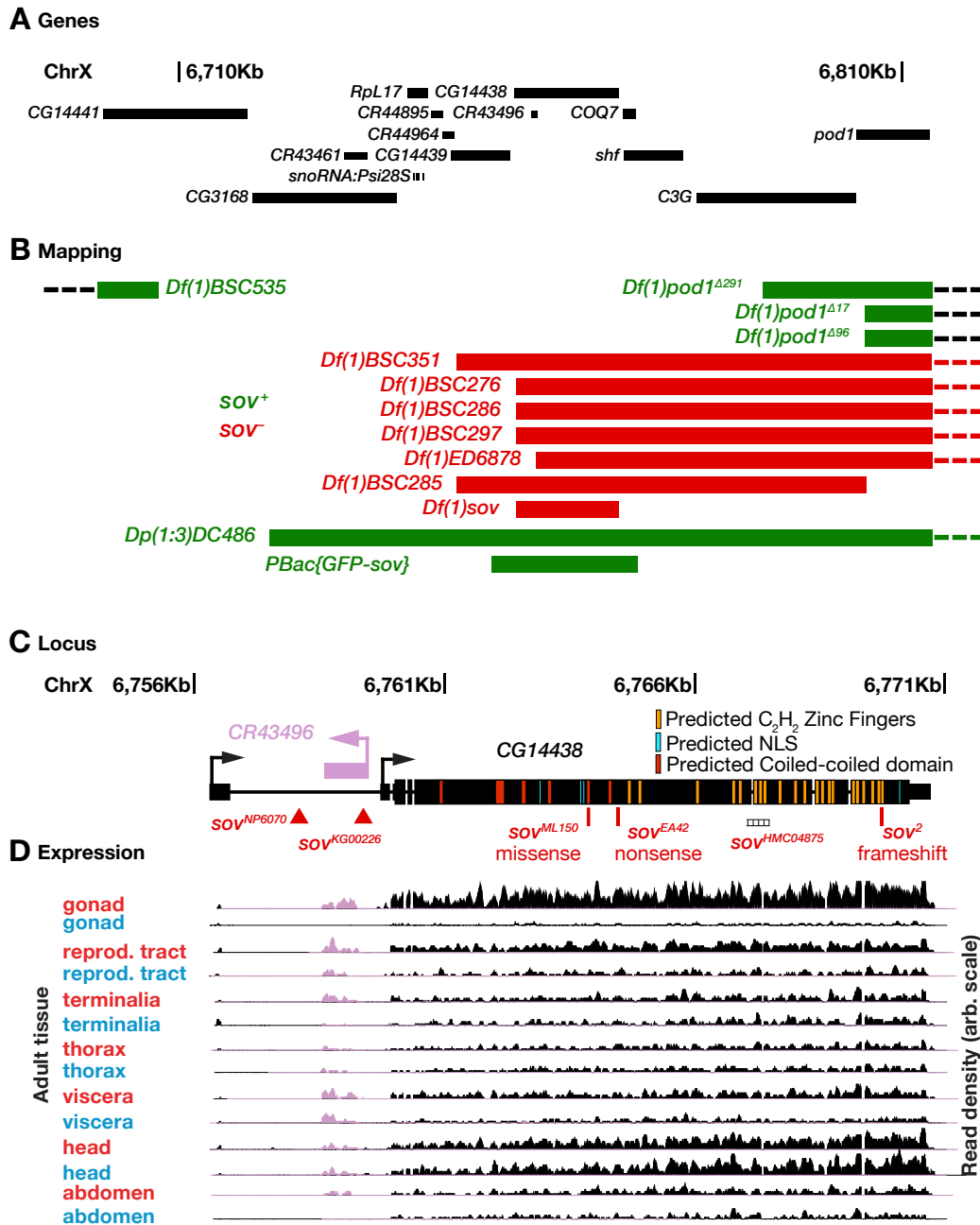
482

483 **Author contributions**

484 LB, KC, BO, and DAL designed the project and analyzed data. LB, KC, CW, and KJTV
485 performed genetics. LB and HY performed genomics. LB, EAC, CW and DAL performed
486 imaging. LB, BO, and DAL wrote the manuscript. All authors reviewed data and provided
487 feedback on the manuscript.

488

Benner_Fig1



489

490

491

492

493

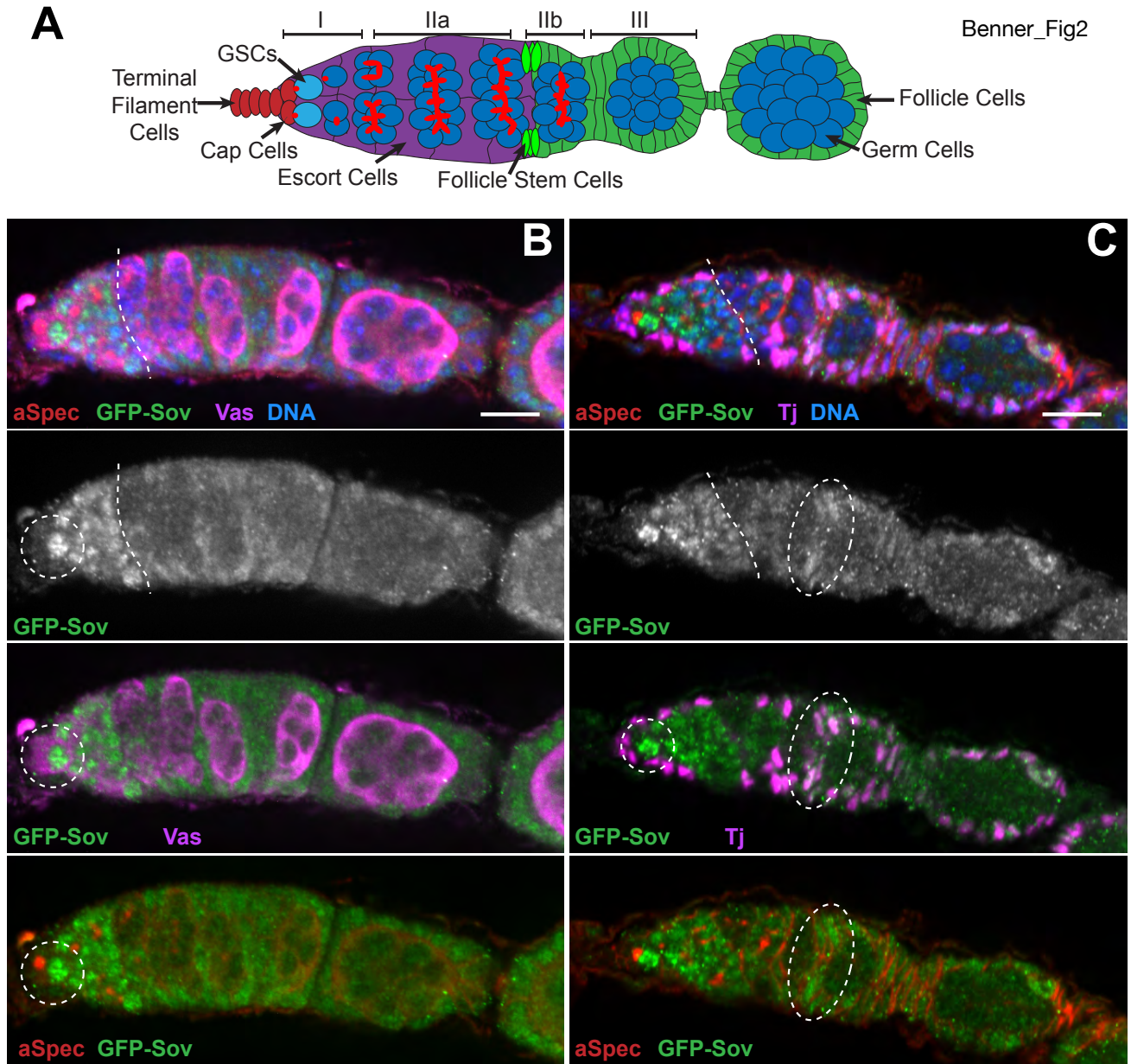
494

495

496

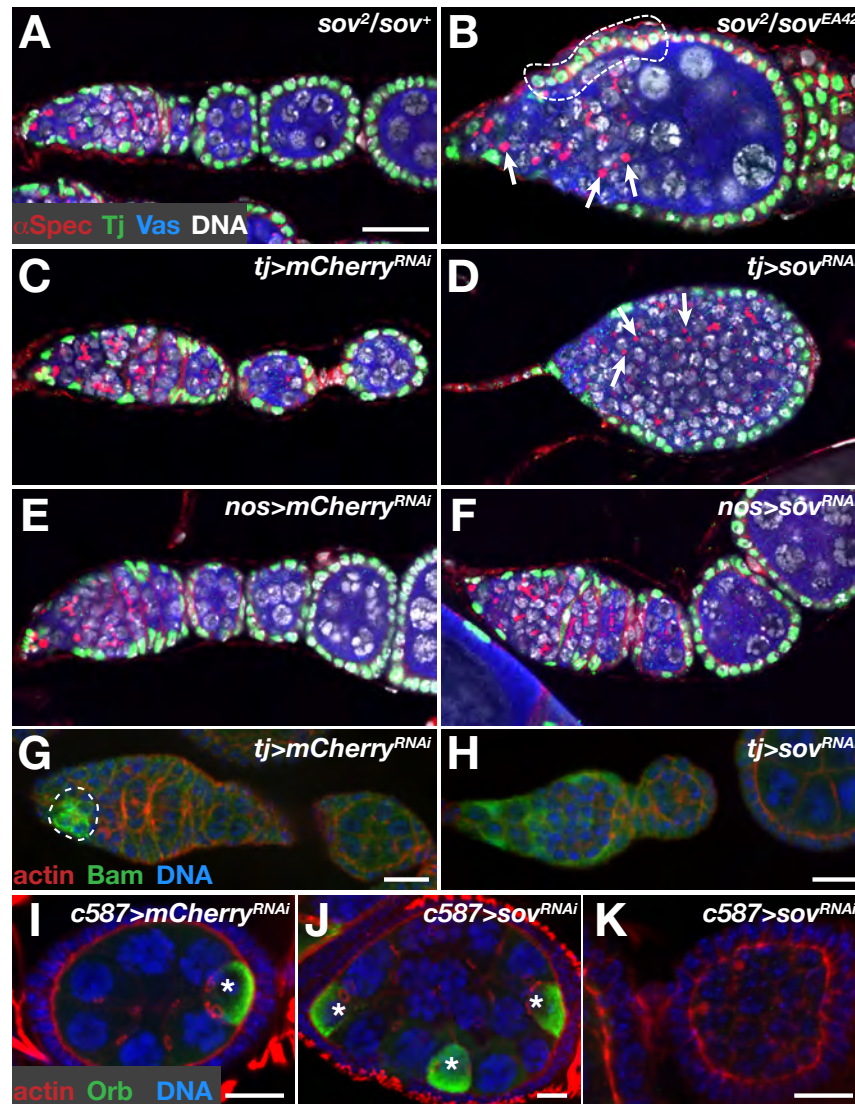
497

Figure 1. *sov* is *CG14438*. (A) Genes of the genomic interval X:6710000–6810000 (Gramates et al. 2017). (B) Deficiency (*Df*) and Duplication (*Dp*) mapping. Noncomplementing (*sov*⁻, red) and complementing (*sov*⁺, green) alleles and rearrangements are shown. (C) Schematic of the *CG14438* (black) and *CR43496* (purple) genes. Transcription start (bent arrows), introns (thin lines) non-coding regions (medium lines) and coding regions (thick lines) are shown. Transposon insertions (triangles), point mutations (red lines), the region targeted by the shRNAi transgene (base-paired), and Sov protein features are shown. (D) RNA expression tracks by tissue type from female (red) or male (blue) adults.



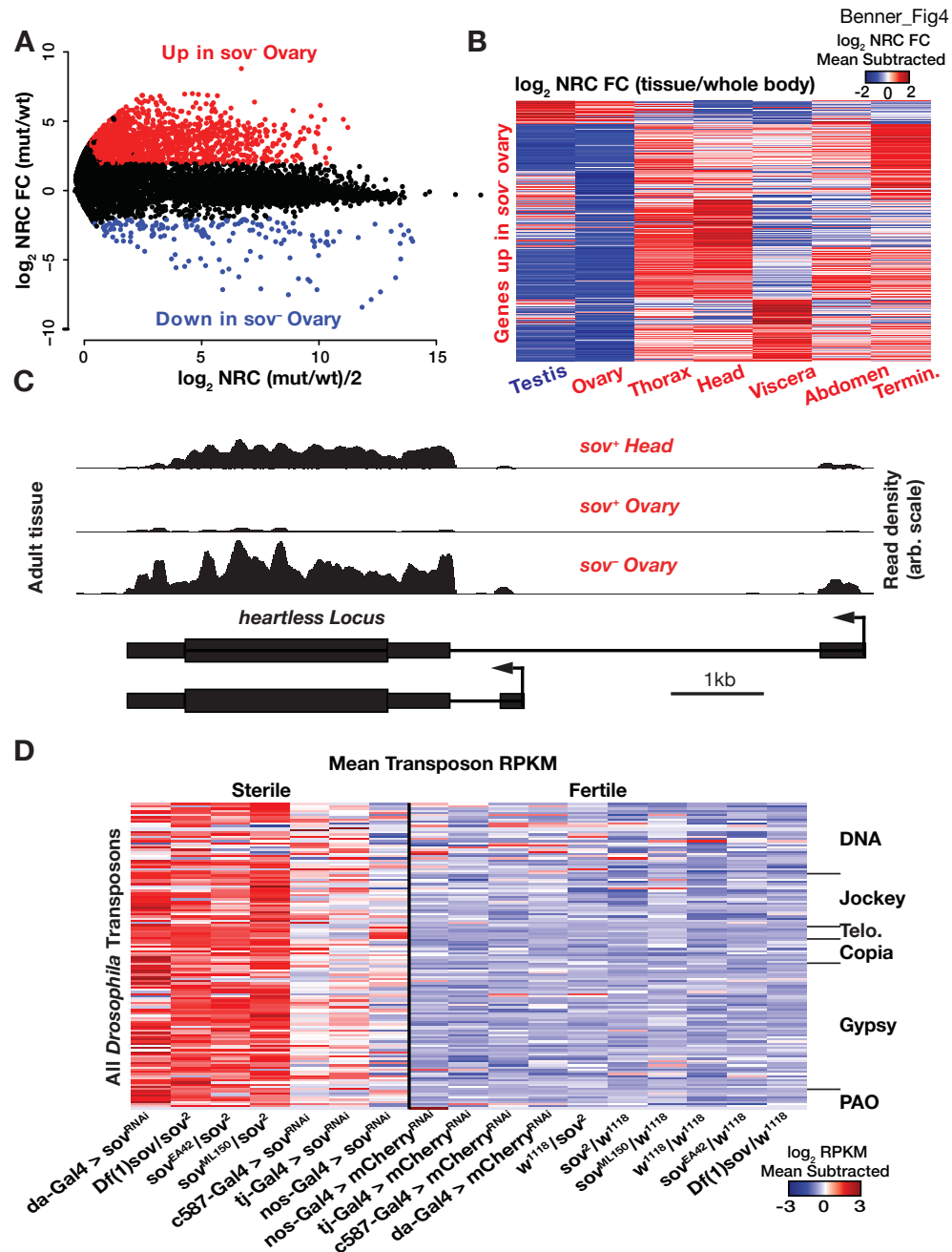
498
499
500
501
502
503

Figure 2. Sov gerarium expression. (A) Cartoon showing gerarium regions I-III and young egg chamber with cell types labeled. (B,C) 1d posteclosion, visualized for GFP-Sov (green), anti- α Spectrin (red). Images show single optical sections. (B) Sov contrasted with anti-Vas germline (magenta), or (C) -Tj somatic staining (magenta). GFP-Sov expression regions of interest (see text) are shown (dashed lines). Bars: 10 μ m.



504
505
506
507
508
509
510
511
512
513

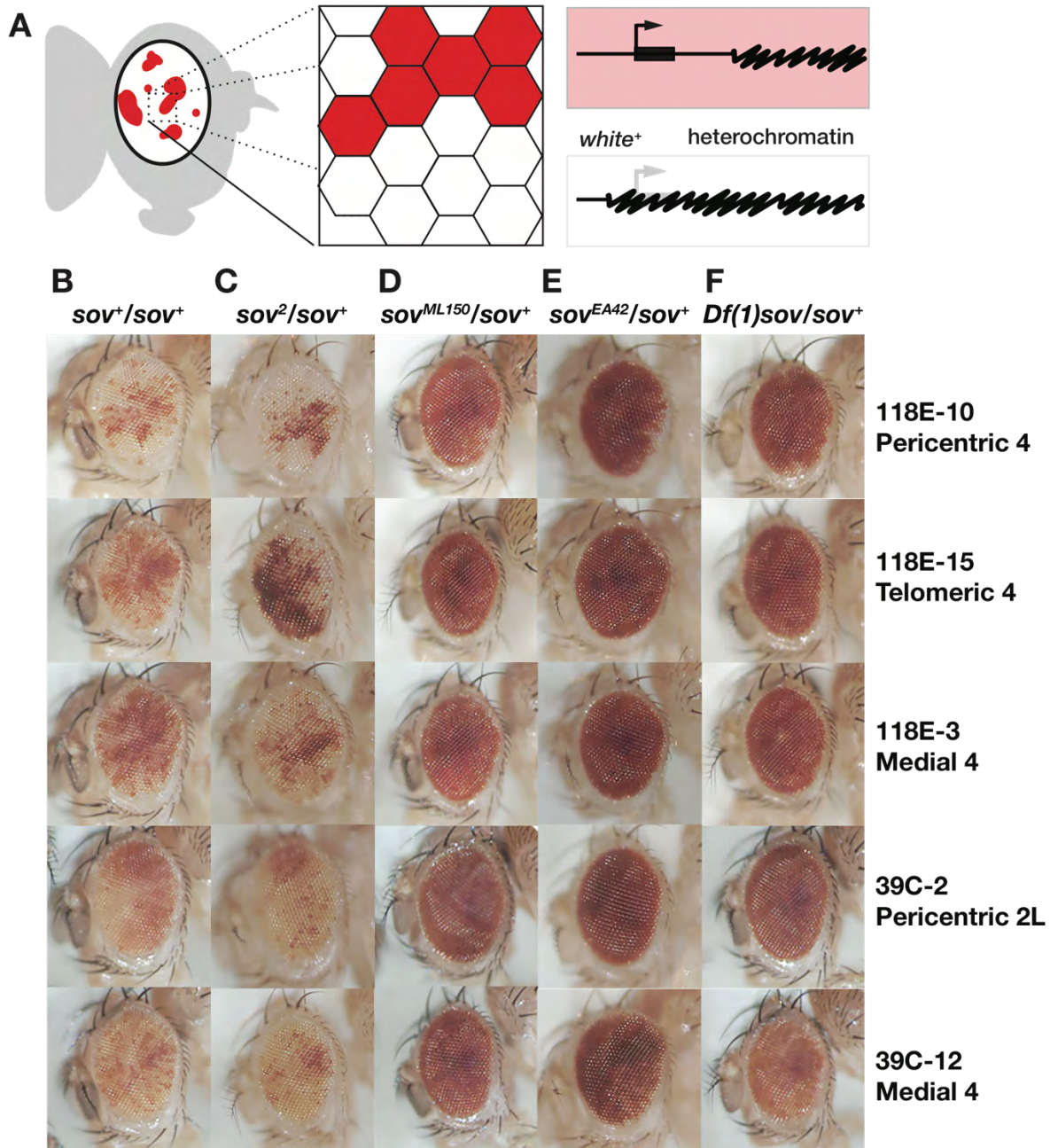
Figure 3. *sov* mutant defects. Immunofluorescence for the indicated probes in the noted genotypes. (A–F) Single optical sections of germaria (4–5d posteclosion) stained with anti-Vas (blue), -Tj (green), - α Spectrin (red), and DAPI (white) with dot spectrosomes (arrows) and displaced follicle cells (dashed lines) shown. (G, H) Single optical sections of germaria (1d posteclosion) stained with anti-Bam (green), -actin (red), and DAPI (blue). Bam region of interest is shown (dashed circles). (I–K) Maximum intensity projections of germaria (1d posteclosion) stained with anti-Orb (green), -actin (red), and DAPI (blue). Orb+ cells shown (*). Bars: (A–F) 20 μ m, (G–K) 10 μ m.



514
 515 **Figure 4. *sov* mutant transcriptome.** (A) Relative expression in *sov*⁻ vs *sov*⁺ ovaries plotted
 516 against the mean expression in both sample types. Units are \log_2 normalized read counts
 517 (NRC). Data points are genes, those with >4-fold change (\log_2 2, red) or <-4 fold change (\log_2
 518 -2, blue) and FDR *padj* value <0.05 are highlighted. (B) Tissue-biased expression in wild type
 519 tissues for genes derepressed in *sov* mutant ovaries. Heatmap from mean-subtracted ratios
 520 scaled across tissues (red=higher; blue=lower). (C) RNA-seq normalized read densities of the
 521 *heartless* locus. (D) Transposable element expression in *sov* mutants (sterile) and controls
 522 (fertile). Heatmap from mean-subtracted reads (in RPKM. red=higher; blue=lower) scaled for
 523 each transposable element (rows) across genotypes (columns). Transposon classes for DNA,
 524 non-LTR (Jockey), telomeric repeat (Telo), and LTR (Gypsy, Copia, and PAO) are indicated.

525

Benner_Fig5



526

527

528

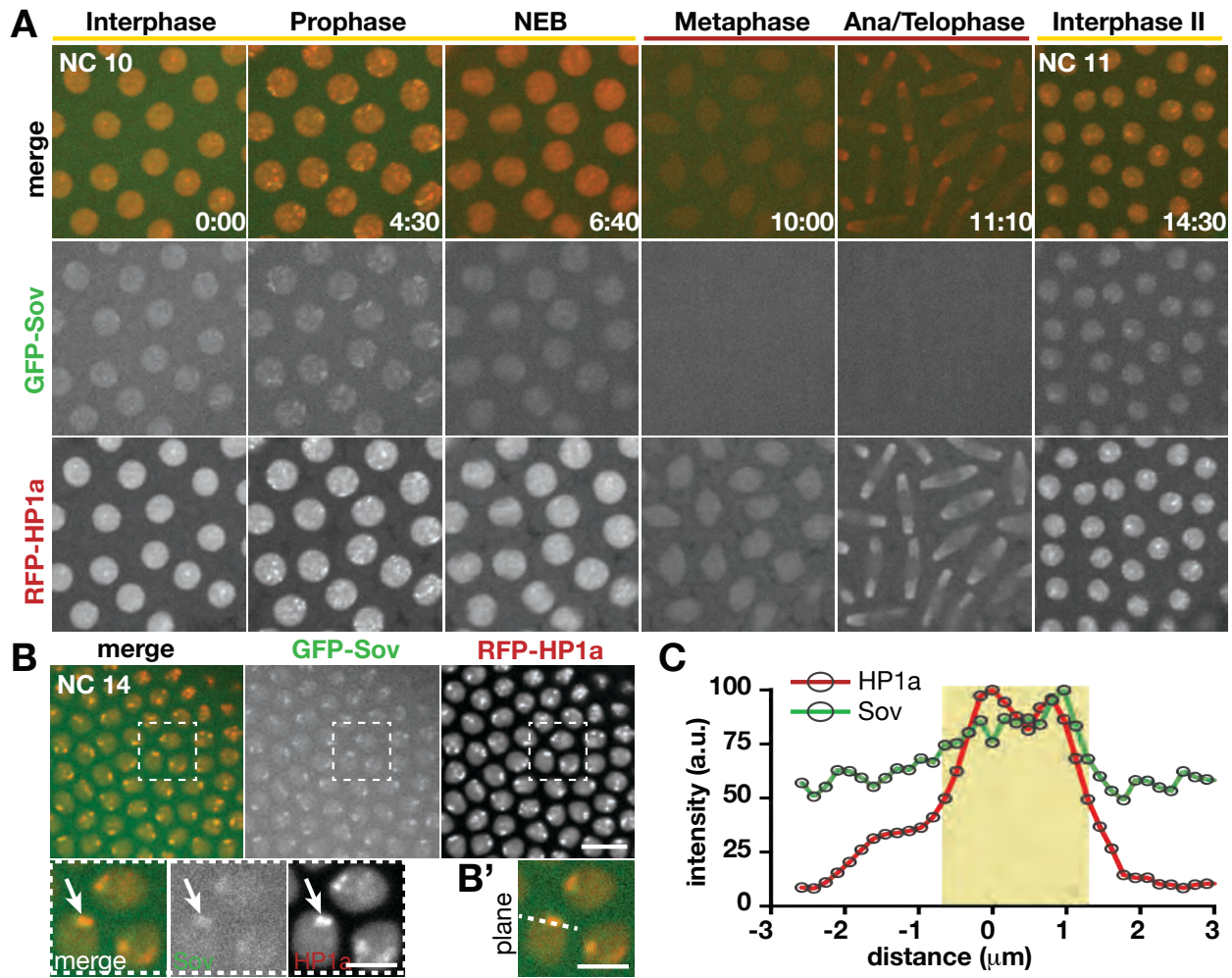
529

530

531

Figure 5. Sov is a dominant suppressor of position effect variegation. (A) Cartoon of position-effect variegation (PEV) in the eye. Expression of the *white* gene (bent arrow, thick bar, red) can be silenced (white) by proximal heterochromatin (squiggled) spreading. (B–F) Eyes from adults of the indicated genotypes (columns) with variegated expression of *P{hsp26-pt-T}* transgenes inserted into the indicated chromosomal positions (rows).

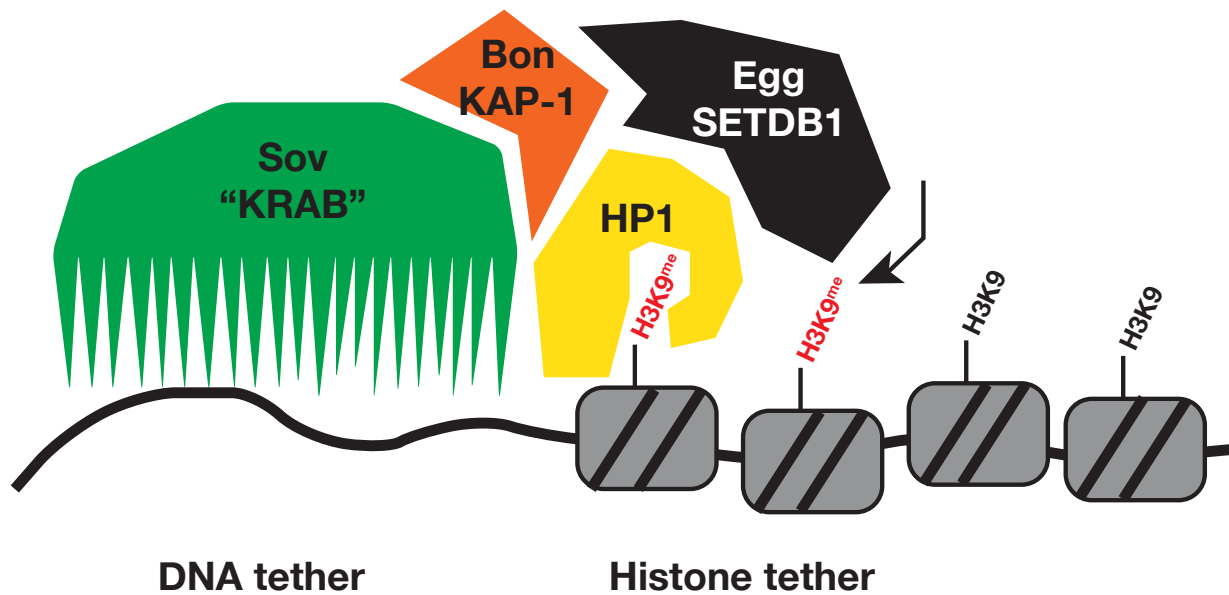
27



532
533
534
535
536
537
538
539
540
541
542
543
544

Figure 6. Sov colocalizes with HP1a. Stills from live imaging of embryos expressing GFP-Sov and RFP-HP1a. (A) Localization of GFP-Sov and RFP-HP1a (rows) in an embryo progressing from NC 10 to 11 with cell cycle stages (columns, nuclear envelope breakdown=NEB) and time (min:s) shown. (B) NC 14 embryo. Boxed regions are magnified in insets below. An HP1a subnuclear domain is shown (arrows). (B') Single optical section containing peak HP1a fluorescence of inset from (B). Dashed line indicates region used for histogram analysis. (A,B) Maximum projections through 1.5 μm volume at 1F/30s. Bars: 10 μm ; insets, 5 μm . (C) Histogram of HP1a and Sov fluorescence intensity measured in (B'). Fluorescence levels (arbitrary units) normalized to the peak fluorescence intensity for each channel and the distance (μm) to peak HP1a signal. Half maximum HP1a fluorescence is shaded (yellow).

Benner_Fig7



545
546
547
548
549
550

Figure 7. Working model of *sov* function. *Sov* protein function and attributes are analogous to the mammalian KRAB proteins (green). Like KRAB proteins, *Sov* is in complex with HP1a (yellow), Bon (mammalian KAP-1, orange) and Egg (mammalian SETDB1, black) providing a DNA tether to stabilize a repressed chromatin state.

551 References

- 552 Alekseyenko, Artyom A., Andrey A. Gorchakov, Barry M. Zee, Stephen M. Fuchs, Peter V. Kharchenko,
553 and Mitzi I. Kuroda. 2014. "Heterochromatin-Associated Interactions of Drosophila HP1a with
554 dADD1, HIP1, and Repetitive RNAs." *Genes & Development* 28 (13): 1445–60.
- 555 Anders, Simon, Paul Theodor Pyl, and Wolfgang Huber. 2015. "HTSeq--a Python Framework to Work
556 with High-Throughput Sequencing Data." *Bioinformatics* 31 (2): 166–69.
- 557 Barton, Lacy J., Kaylee E. Lovander, Belinda S. Pinto, and Pamela K. Geyer. 2016. "Drosophila Male
558 and Female Germline Stem Cell Niches Require the Nuclear Lamina Protein Otefin."
559 *Developmental Biology* 415 (1): 75–86.
- 560 Bausek, Nina. 2013. "JAK-STAT Signaling in Stem Cells and Their Niches in Drosophila." *JAK-STAT* 2
561 (3): e25686.
- 562 Beckstead, R. B., S. S. Ner, K. G. Hales, T. A. Grigliatti, B. S. Baker, and H. J. Bellen. 2005. "Bonus, a
563 Drosophila TIF1 Homolog, Is a Chromatin-Associated Protein That Acts as a Modifier of Position-
564 Effect Variegation." *Genetics* 169 (2): 783–94.
- 565 Bindea, Gabriela, Bernhard Mlecnik, Hubert Hackl, Pornpimol Charoentong, Marie Tosolini, Amos
566 Kirilovsky, Wolf-Herman Fridman, Franck Pagès, Zlatko Trajanoski, and Jérôme Galon. 2009.
567 "ClueGO: A Cytoscape Plug-in to Decipher Functionally Grouped Gene Ontology and Pathway
568 Annotation Networks." *Bioinformatics* 25 (8): 1091–93.
- 569 Börner, Kenneth, Dhawal Jain, Paula Vazquez-Pianzola, Sandra Vengadasalam, Natascha Steffen,
570 Dmitry V. Fyodorov, Pavel Tomancak, Alexander Konev, Beat Suter, and Peter B. Becker. 2016.
571 "A Role for Tuned Levels of Nucleosome Remodeler Subunit ACF1 during Drosophila Oogenesis."
572 *Developmental Biology* 411 (2): 217–30.
- 573 Brennecke, Julius, Alexei A. Aravin, Alexander Stark, Monica Dus, Manolis Kellis, Ravi
574 Sachidanandam, and Gregory J. Hannon. 2007. "Discrete Small RNA-Generating Loci as Master
575 Regulators of Transposon Activity in Drosophila." *Cell* 128 (6): 1089–1103.
- 576 Brown, James B., Nathan Boley, Robert Eisman, Gemma E. May, Marcus H. Stoiber, Michael O. Duff,
577 Ben W. Booth, et al. 2014. "Diversity and Dynamics of the Drosophila Transcriptome." *Nature* 512
578 (7515): 393–99.
- 579 Brown, J. Lesley, Cornelia Fritsch, Jürg Mueller, and Judith A. Kassis. 2003. "The Drosophila Pho-like
580 Gene Encodes a YY1-Related DNA Binding Protein That Is Redundant with Pleiohomeotic in
581 Homeotic Gene Silencing." *Development* 130 (2): 285–94.
- 582 Casper, Jonathan, Ann S. Zweig, Chris Villarreal, Cath Tyner, Matthew L. Speir, Kate R. Rosenbloom,
583 Brian J. Raney, et al. 2018. "The UCSC Genome Browser Database: 2018 Update." *Nucleic Acids*
584 *Research* 46 (D1): D762–69.
- 585 Chen, Shuyi, Su Wang, and Ting Xie. 2011. "Restricting Self-Renewal Signals within the Stem Cell
586 Niche: Multiple Levels of Control." *Current Opinion in Genetics & Development* 21 (6): 684–89.
- 587 Chen, Taiping, and Sharon Y. R. Dent. 2014. "Chromatin Modifiers and Remodellers: Regulators of
588 Cellular Differentiation." *Nature Reviews. Genetics* 15 (2): 93–106.
- 589 Chou, T. B., and N. Perrimon. 1996. "The Autosomal FLP-DFS Technique for Generating Germline
590 Mosaics in Drosophila Melanogaster." *Genetics* 144 (4): 1673–79.
- 591 Cingolani, Pablo, Adrian Platts, Le Lily Wang, Melissa Coon, Tung Nguyen, Luan Wang, Susan J.
592 Land, Xiangyi Lu, and Douglas M. Ruden. 2012. "A Program for Annotating and Predicting the
593 Effects of Single Nucleotide Polymorphisms, SnpEff: SNPs in the Genome of Drosophila
594 Melanogaster Strain w1118; Iso-2; Iso-3." *Fly* 6 (2): 80–92.
- 595 Clark, R. F., and S. C. Elgin. 1992. "Heterochromatin Protein 1, a Known Suppressor of Position-Effect
596 Variegation, Is Highly Conserved in Drosophila." *Nucleic Acids Research* 20 (22): 6067–74.
- 597 Clough, Emily, Woongjoon Moon, Shengxian Wang, Kathleen Smith, and Tulle Hazelrigg. 2007.
598 "Histone Methylation Is Required for Oogenesis in Drosophila." *Development* 134 (1): 157–65.
- 599 Clough, Emily, Thomas Tedeschi, and Tulle Hazelrigg. 2014. "Epigenetic Regulation of Oogenesis and
600 Germ Stem Cell Maintenance by the Drosophila Histone Methyltransferase Eggless/dSetDB1."

- 601 *Developmental Biology* 388 (2): 181–91.
- 602 Cook, R. Kimberley, Stacey J. Christensen, Jennifer A. Deal, Rachel A. Coburn, Megan E. Deal, Jill M.
- 603 Gresens, Thomas C. Kaufman, and Kevin R. Cook. 2012. “The Generation of Chromosomal
- 604 Deletions to Provide Extensive Coverage and Subdivision of the *Drosophila Melanogaster*
- 605 Genome.” *Genome Biology* 13 (3): R21.
- 606 Court, Donald L., Srividya Swaminathan, Daiguan Yu, Helen Wilson, Teresa Baker, Mikail Bubunenکو,
- 607 James Sawitzke, and Shyam K. Sharan. 2003. “Mini-Lambda: A Tractable System for
- 608 Chromosome and BAC Engineering.” *Gene* 315 (October): 63–69.
- 609 Di Stefano, Luisa, Jun-Yuan Ji, Nam-Sung Moon, Anabel Herr, and Nicholas Dyson. 2007. “Mutation of
- 610 *Drosophila* Lsd1 Disrupts H3-K4 Methylation, Resulting in Tissue-Specific Defects during
- 611 Development.” *Current Biology: CB* 17 (9): 808–12.
- 612 Ebert, Anja, Sandro Lein, Gunnar Schotta, and Gunter Reuter. 2006. “Histone Modification and the
- 613 Control of Heterochromatin Gene Silencing in *Drosophila*.” *Chromosome Research: An*
- 614 *International Journal on the Molecular, Supramolecular and Evolutionary Aspects of Chromosome*
- 615 *Biology* 14 (4): 377–92.
- 616 Ecco, Gabriela, Michael Imbeault, and Didier Trono. 2017. “KRAB Zinc Finger Proteins.” *Development*
- 617 144 (15): 2719–29.
- 618 Eissenberg, J. C., T. C. James, D. M. Foster-Hartnett, T. Hartnett, V. Ngan, and S. C. Elgin. 1990.
- 619 “Mutation in a Heterochromatin-Specific Chromosomal Protein Is Associated with Suppression of
- 620 Position-Effect Variegation in *Drosophila Melanogaster*.” *Proceedings of the National Academy of*
- 621 *Sciences of the United States of America* 87 (24): 9923–27.
- 622 Elgin, Sarah C. R., and Gunter Reuter. 2013. “Position-Effect Variegation, Heterochromatin Formation,
- 623 and Gene Silencing in *Drosophila*.” *Cold Spring Harbor Perspectives in Biology* 5 (8): a017780.
- 624 Eliazer, Susan, Victor Palacios, Zhaohui Wang, Rahul K. Kollipara, Ralf Kittler, and Michael Buszczak.
- 625 2014. “Lsd1 Restricts the Number of Germline Stem Cells by Regulating Multiple Targets in Escort
- 626 Cells.” *PLoS Genetics* 10 (3): e1004200.
- 627 Eliazer, Susan, Nevine A. Shalaby, and Michael Buszczak. 2011. “Loss of Lysine-Specific Demethylase
- 628 1 Nonautonomously Causes Stem Cell Tumors in the *Drosophila* Ovary.” *Proceedings of the*
- 629 *National Academy of Sciences of the United States of America* 108 (17): 7064–69.
- 630 Foe, V. E., and B. M. Alberts. 1983. “Studies of Nuclear and Cytoplasmic Behaviour during the Five
- 631 Mitotic Cycles That Precede Gastrulation in *Drosophila* Embryogenesis.” *Journal of Cell Science*
- 632 61 (May): 31–70.
- 633 Fuller, Margaret T., and Allan C. Spradling. 2007. “Male and Female *Drosophila* Germline Stem Cells:
- 634 Two Versions of Immortality.” *Science* 316 (5823): 402–4.
- 635 Gene Ontology Consortium. 2015. “Gene Ontology Consortium: Going Forward.” *Nucleic Acids*
- 636 *Research* 43 (Database issue): D1049–56.
- 637 Gilboa, Lilach. 2015. “Organizing Stem Cell Units in the *Drosophila* Ovary.” *Current Opinion in Genetics*
- 638 *& Development* 32 (June): 31–36.
- 639 Goode, S., D. Wright, and A. P. Mahowald. 1992. “The Neurogenic Locus Brainiac Cooperates with the
- 640 *Drosophila* EGF Receptor to Establish the Ovarian Follicle and to Determine Its Dorsal-Ventral
- 641 Polarity.” *Development* 116 (1): 177–92.
- 642 Gramates, L. Sian, Steven J. Marygold, Gilberto Dos Santos, Jose-Maria Urbano, Giulia Antonazzo,
- 643 Beverley B. Matthews, Alix J. Rey, et al. 2017. “FlyBase at 25: Looking to the Future.” *Nucleic*
- 644 *Acids Research* 45 (D1): D663–71.
- 645 Graveley, Brenton R., Angela N. Brooks, Joseph W. Carlson, Michael O. Duff, Jane M. Landolin, Li
- 646 Yang, Carlo G. Artieri, et al. 2011. “The Developmental Transcriptome of *Drosophila*
- 647 *Melanogaster*.” *Nature* 471 (7339): 473–79.
- 648 Gu, Tingting, and Sarah C. R. Elgin. 2013. “Maternal Depletion of Piwi, a Component of the RNAi
- 649 System, Impacts Heterochromatin Formation in *Drosophila*.” *PLoS Genetics* 9 (9): e1003780.
- 650 Hsieh, M., Y. Tintut, and J. D. Gralla. 1994. “Functional Roles for the Glutamines within the Glutamine-
- 651 Rich Region of the Transcription Factor Sigma 54.” *The Journal of Biological Chemistry* 269 (1):

- 652 373–78.
- 653 Huang, Audrey M., E. Jay Rehm, and Gerald M. Rubin. 2009. “Quick Preparation of Genomic DNA
654 from *Drosophila*.” *Cold Spring Harbor Protocols* 2009 (4): db.prot5198.
- 655 James, T. C., and S. C. Elgin. 1986. “Identification of a Nonhistone Chromosomal Protein Associated
656 with Heterochromatin in *Drosophila Melanogaster* and Its Gene.” *Molecular and Cellular Biology* 6
657 (11): 3862–72.
- 658 Jankovics, Ferenc, László Henn, Ágnes Bujna, Péter Vilmos, Kerstin Spirohn, Michael Boutros, and
659 Miklós Erdélyi. 2014. “Functional Analysis of the *Drosophila* Embryonic Germ Cell Transcriptome
660 by RNA Interference.” *PloS One* 9 (6): e98579.
- 661 Jenuwein, T., and C. D. Allis. 2001. “Translating the Histone Code.” *Science* 293 (5532): 1074–80.
- 662 Jiang, Lichun, Felix Schlesinger, Carrie A. Davis, Yu Zhang, Renhua Li, Marc Salit, Thomas R.
663 Gingeras, and Brian Oliver. 2011. “Synthetic Spike-in Standards for RNA-Seq Experiments.”
664 *Genome Research* 21 (9): 1543–51.
- 665 Kassis, Judith A., James A. Kennison, and John W. Tamkun. 2017. “Polycomb and Trithorax Group
666 Genes in *Drosophila*.” *Genetics* 206 (4): 1699–1725.
- 667 Kent, W. James, Charles W. Sugnet, Terrence S. Furey, Krishna M. Roskin, Tom H. Pringle, Alan M.
668 Zahler, and David Haussler. 2002. “The Human Genome Browser at UCSC.” *Genome Research*
669 12 (6): 996–1006.
- 670 Kim, Daehwan, Ben Langmead, and Steven L. Salzberg. 2015. “HISAT: A Fast Spliced Aligner with
671 Low Memory Requirements.” *Nature Methods* 12 (4): 357–60.
- 672 Kouzarides, Tony. 2007. “Chromatin Modifications and Their Function.” *Cell* 128 (4): 693–705.
- 673 Lantz, V., J. S. Chang, J. I. Horabin, D. Bopp, and P. Schedl. 1994. “The *Drosophila* Orb RNA-Binding
674 Protein Is Required for the Formation of the Egg Chamber and Establishment of Polarity.” *Genes &
675 Development* 8 (5): 598–613.
- 676 Leader, David P., Sue A. Krause, Aniruddha Pandit, Shireen A. Davies, and Julian A. T. Dow. 2018.
677 “FlyAtlas 2: A New Version of the *Drosophila Melanogaster* Expression Atlas with RNA-Seq,
678 miRNA-Seq and Sex-Specific Data.” *Nucleic Acids Research* 46 (D1): D809–15.
- 679 Lee, Hangnoh, Dong-Yeon Cho, Cale Whitworth, Robert Eisman, Melissa Phelps, John Roote, Thomas
680 Kaufman, et al. 2016. “Effects of Gene Dose, Chromatin, and Network Topology on Expression in
681 *Drosophila Melanogaster*.” *PLoS Genetics* 12 (9): e1006295.
- 682 Lee, Hangnoh, P. Scott Pine, Jennifer McDaniel, Marc Salit, and Brian Oliver. 2016. “External RNA
683 Controls Consortium Beta Version Update.” *Journal of Genomics* 4 (July): 19–22.
- 684 Lee, Jeannie T. 2009. “Lessons from X-Chromosome Inactivation: Long ncRNA as Guides and Tethers
685 to the Epigenome.” *Genes & Development* 23 (16): 1831–42.
- 686 Lerit, Dorothy A., Holly A. Jordan, John S. Poulton, Carey J. Fagerstrom, Brian J. Galletta, Mark Peifer,
687 and Nasser M. Rusan. 2015. “Interphase Centrosome Organization by the PLP-Cnn Scaffold Is
688 Required for Centrosome Function.” *The Journal of Cell Biology* 210 (1): 79–97.
- 689 Li, Heng. 2011. “A Statistical Framework for SNP Calling, Mutation Discovery, Association Mapping and
690 Population Genetical Parameter Estimation from Sequencing Data.” *Bioinformatics* 27 (21): 2987–
691 93.
- 692 Li, Heng, Bob Handsaker, Alec Wysoker, Tim Fennell, Jue Ruan, Nils Homer, Gabor Marth, Goncalo
693 Abecasis, Richard Durbin, and 1000 Genome Project Data Processing Subgroup. 2009. “The
694 Sequence Alignment/Map Format and SAMtools.” *Bioinformatics* 25 (16): 2078–79.
- 695 Lin, H., and A. C. Spradling. 1995. “Fusome Asymmetry and Oocyte Determination in *Drosophila*.”
696 *Developmental Genetics* 16 (1): 6–12.
- 697 Li, Xuanying, Christopher W. Seidel, Leanne T. Szerszen, Jeffrey J. Lange, Jerry L. Workman, and
698 Susan M. Abmayr. 2017. “Enzymatic Modules of the SAGA Chromatin-Modifying Complex Play
699 Distinct Roles in *Drosophila* Gene Expression and Development.” *Genes & Development* 31 (15):
700 1588–1600.
- 701 Lorch, Yahli, and Roger D. Kornberg. 2017. “Chromatin-Remodeling for Transcription.” *Quarterly
702 Reviews of Biophysics* 50 (January): e5.

- 703 Love, Michael I., Wolfgang Huber, and Simon Anders. 2014. "Moderated Estimation of Fold Change
704 and Dispersion for RNA-Seq Data with DESeq2." *Genome Biology* 15 (12): 550.
- 705 Mason, James M., Radmila Capkova Frydrychova, and Harald Biessmann. 2008. "Drosophila
706 Telomeres: An Exception Providing New Insights." *BioEssays: News and Reviews in Molecular,
707 Cellular and Developmental Biology* 30 (1): 25–37.
- 708 McConnell, Kristopher H., Michael Dixon, and Brian R. Calvi. 2012. "The Histone Acetyltransferases
709 CBP and Chameau Integrate Developmental and DNA Replication Programs in Drosophila
710 Ovarian Follicle Cells." *Development* 139 (20): 3880–90.
- 711 McKearin, D. M., and A. C. Spradling. 1990. "Bag-of-Marbles: A Drosophila Gene Required to Initiate
712 Both Male and Female Gametogenesis." *Genes & Development* 4 (12B): 2242–51.
- 713 McKearin, D., and B. Ohlstein. 1995. "A Role for the Drosophila Bag-of-Marbles Protein in the
714 Differentiation of Cystoblasts from Germline Stem Cells." *Development* 121 (9): 2937–47.
- 715 Mohler, Dawson, and Andrea Carroll. 1984. "Report of Dawson Mohler and Andrea Carroll." *Drosophila
716 Information Service* 60 (June): 236–41.
- 717 Mohler, J. D. 1977. "Developmental Genetics of the Drosophila Egg. I. Identification of 59 Sex-Linked
718 Cistrons with Maternal Effects on Embryonic Development." *Genetics* 85 (2): 259–72.
- 719 Ohlstein, B., and D. McKearin. 1997. "Ectopic Expression of the Drosophila Bam Protein Eliminates
720 Oogenic Germline Stem Cells." *Development* 124 (18): 3651–62.
- 721 Orr-Weaver, T. L. 1991. "Drosophila Chorion Genes: Cracking the Eggshell's Secrets." *BioEssays:
722 News and Reviews in Molecular, Cellular and Developmental Biology* 13 (3): 97–105.
- 723 Parks, Annette L., Kevin R. Cook, Marcia Belvin, Nicholas A. Dompe, Robert Fawcett, Kari Huppert,
724 Lory R. Tan, et al. 2004. "Systematic Generation of High-Resolution Deletion Coverage of the
725 Drosophila Melanogaster Genome." *Nature Genetics* 36 (3): 288–92.
- 726 Peng, Jany C., Anton Valouev, Na Liu, and Haifan Lin. 2016. "Piwi Maintains Germline Stem Cells and
727 Oogenesis in Drosophila through Negative Regulation of Polycomb Group Proteins." *Nature
728 Genetics* 48 (3): 283–91.
- 729 Pine, P. Scott, Sarah A. Munro, Jerod R. Parsons, Jennifer McDaniel, Anne Bergstrom Lucas, Jean
730 Lozach, Timothy G. Myers, Qin Su, Sarah M. Jacobs-Helber, and Marc Salit. 2016. "Evaluation of
731 the External RNA Controls Consortium (ERCC) Reference Material Using a Modified Latin Square
732 Design." *BMC Biotechnology* 16 (1): 54.
- 733 Quinlan, Aaron R., and Ira M. Hall. 2010. "BEDTools: A Flexible Suite of Utilities for Comparing
734 Genomic Features." *Bioinformatics* 26 (6): 841–42.
- 735 R Core Team. 2017. "A Language and Environment for Statistical Computing." Vienna, Austria: R
736 Foundation for Statistical Computing. <https://www.R-project.org/>.
- 737 Reuter, G., and P. Spierer. 1992. "Position Effect Variegation and Chromatin Proteins." *BioEssays:
738 News and Reviews in Molecular, Cellular and Developmental Biology* 14 (9): 605–12.
- 739 Robinson, Scott W., Pawel Herzyk, Julian A. T. Dow, and David P. Leader. 2013. "FlyAtlas: Database
740 of Gene Expression in the Tissues of Drosophila Melanogaster." *Nucleic Acids Research* 41
741 (Database issue): D744–50.
- 742 Rudolph, Thomas, Masato Yonezawa, Sandro Lein, Kathleen Heidrich, Stefan Kubicek, Christiane
743 Schäfer, Sameer Phalke, et al. 2007. "Heterochromatin Formation in Drosophila Is Initiated through
744 Active Removal of H3K4 Methylation by the LSD1 Homolog SU(VAR)3-3." *Molecular Cell* 26 (1):
745 103–15.
- 746 Sambrook, Joseph, and David W. Russell. 2006. "Purification of Nucleic Acids by Extraction with
747 Phenol:chloroform." *CSH Protocols* 2006 (1). <https://doi.org/10.1101/pdb.prot4455>.
- 748 Shannon, Paul, Andrew Markiel, Owen Ozier, Nitin S. Baliga, Jonathan T. Wang, Daniel Ramage, Nada
749 Amin, Benno Schwikowski, and Trey Ideker. 2003. "Cytoscape: A Software Environment for
750 Integrated Models of Biomolecular Interaction Networks." *Genome Research* 13 (11): 2498–2504.
- 751 Smit, Afa, R. Hubley, and P. Green. 2013-2015. "RepeatMasker Open-4.0."
752 <http://www.repeatmasker.org>.
- 753 Soshnev, Alexey A., Ryan M. Baxley, J. Robert Manak, Kai Tan, and Pamela K. Geyer. 2013. "The

- 754 Insulator Protein Suppressor of Hairy-Wing Is an Essential Transcriptional Repressor in the
755 *Drosophila* Ovary." *Development* 140 (17): 3613–23.
- 756 Stork, Tobias, Amy Sheehan, Ozge E. Tasdemir-Yilmaz, and Marc R. Freeman. 2014. "Neuron-Glia
757 Interactions through the Heartless FGF Receptor Signaling Pathway Mediate Morphogenesis of
758 *Drosophila* Astrocytes." *Neuron* 83 (2): 388–403.
- 759 Teixeira, Felipe Karam, Martyna Okuniewska, Colin D. Malone, Rémi-Xavier Coux, Donald C. Rio, and
760 Ruth Lehmann. 2017. "piRNA-Mediated Regulation of Transposon Alternative Splicing in the Soma
761 and Germ Line." *Nature* 552 (7684): 268–72.
- 762 Teo, Ryan Yee Wei, Amit Anand, Vishweshwaren Sridhar, Katsutomo Okamura, and Toshie Kai. 2018.
763 "Heterochromatin Protein 1a Functions for piRNA Biogenesis Predominantly from Pericentric and
764 Telomeric Regions in *Drosophila*." *Nature Communications* 9 (1): 1735.
- 765 Venken, Koen J. T., Joseph W. Carlson, Karen L. Schulze, Hongling Pan, Yuchun He, Rebecca
766 Spokony, Kenneth H. Wan, et al. 2009. "Versatile P[acman] BAC Libraries for Transgenesis
767 Studies in *Drosophila Melanogaster*." *Nature Methods* 6 (6): 431–34.
- 768 Venken, Koen J. T., Karen L. Schulze, Nele A. Haelterman, Hongling Pan, Yuchun He, Martha Evans-
769 Holm, Joseph W. Carlson, et al. 2011. "MiMIC: A Highly Versatile Transposon Insertion Resource
770 for Engineering *Drosophila Melanogaster* Genes." *Nature Methods* 8 (9): 737–43.
- 771 Vermaak, Danielle, and Harmit S. Malik. 2009. "Multiple Roles for Heterochromatin Protein 1 Genes in
772 *Drosophila*." *Annual Review of Genetics* 43: 467–92.
- 773 Wang, Xiaoxi, Lei Pan, Su Wang, Jian Zhou, William McDowell, Jungeun Park, Jeff Haug, Karen
774 Staehling, Hong Tang, and Ting Xie. 2011. "Histone H3K9 Trimethylase Eggless Controls
775 Germline Stem Cell Maintenance and Differentiation." *PLoS Genetics* 7 (12): e1002426.
- 776 Warming, Søren, Nina Costantino, Donald L. Court, Nancy A. Jenkins, and Neal G. Copeland. 2005.
777 "Simple and Highly Efficient BAC Recombineering Using galK Selection." *Nucleic Acids Research*
778 33 (4): e36.
- 779 Wayne, S., K. Liggett, J. Pettus, and R. N. Nagoshi. 1995. "Genetic Characterization of Small Ovaries,
780 a Gene Required in the Soma for the Development of the *Drosophila* Ovary and the Female
781 Germline." *Genetics* 139 (3): 1309–20.
- 782 Weiler, K. S., and B. T. Wakimoto. 1995. "Heterochromatin and Gene Expression in *Drosophila*."
783 *Annual Review of Genetics* 29: 577–605.
- 784 Yang, Peng, Yixuan Wang, and Todd S. Macfarlan. 2017. "The Role of KRAB-ZFPs in Transposable
785 Element Repression and Mammalian Evolution." *Trends in Genetics: TIG* 33 (11): 871–81.
- 786 Yasuhara, Jiro C., and Barbara T. Wakimoto. 2006. "Oxymoron No More: The Expanding World of
787 Heterochromatic Genes." *Trends in Genetics: TIG* 22 (6): 330–38.
- 788 Yin, Hang, and Haifan Lin. 2007. "An Epigenetic Activation Role of Piwi and a Piwi-Associated piRNA in
789 *Drosophila Melanogaster*." *Nature* 450 (7167): 304–8.
- 790 Yoshioka, K., H. Honma, M. Zushi, S. Kondo, S. Togashi, T. Miyake, and T. Shiba. 1990. "Virus-like
791 Particle Formation of *Drosophila* Copia through Autocatalytic Processing." *The EMBO Journal* 9
792 (2): 535–41.
- 793 Yuan, Kai, and Patrick H. O'Farrell. 2016. "TALE-Light Imaging Reveals Maternally Guided,
794 H3K9me2/3-Independent Emergence of Functional Heterochromatin in *Drosophila* Embryos."
795 *Genes & Development* 30 (5): 579–93.
- 796 Zook, Justin M., Daniel Samarov, Jennifer McDaniel, Shurjo K. Sen, and Marc Salit. 2012. "Synthetic
797 Spike-in Standards Improve Run-Specific Systematic Error Analysis for DNA and RNA
798 Sequencing." *PloS One* 7 (7): e41356.